

SIMULATION OF ENTRAINED FLOW HYDROPYROLYSIS REACTORS

A. Goyal
Institute of Gas Technology
Chicago, Illinois 60616

D. Gidaspo
Chemical Engineering Department
Illinois Institute of Technology
Chicago, Illinois 60616

The phenomena of coal pyrolysis and hydroxyrolysis have become of considerable interest in recent years because of their significance in the efficient conversion of coals to clean fuels. The proposed hydroxyrolysis commercial reactors are usually based on the entrained flow concept in which coal particles are rapidly heated in a dilute phase by mixing with hot hydrogen (or a gas mixture rich in hydrogen). A wide variation in the product distribution can be obtained in such reactors by manipulating temperature, residence time, and other operating parameters. Mathematical models incorporating hydrodynamics, coal kinetics, heat transfer characteristics, etc. are needed for understanding the influence of design variables, feed materials, and process conditions on the reactor performance. The literature is lacking in coal hydroxyrolysis entrained flow reactor models. Such a model has been developed in this study.

Mathematical Formulation

A one-dimensional mathematical model has been formulated here. The physical system considered is an entrained flow hydroxyrolysis reactor. Pulverized coal mixes with the hot gas feed at the reactor entrance. As coal particles are carried by the gas, their temperature increases and hydroxyrolysis takes place.

The single coal particle hydroxyrolysis kinetic model used in this study is described by Goyal (1). The model is primarily based on Johnson's kinetic model (2, 3, 4) supplemented by Suuberg's kinetic model (5) for rapid reactions. In this model, the coal is assumed to consist of eleven solid species while the gas of nine species (Table 1). Gaseous species $(CH_2)_a$ represents gaseous heavy hydrocarbons while $(CH_M)_b$ represents vaporized oils and tars.

The kinetic model has been combined here with reactor flow model and heat and mass transfer characteristics of the multiparticle system to derive a reactor model. Because of the significant amount of coal weight loss and gas generation in such systems, hydrodynamics may also be very important. The equations describing the system are given in Table 2. In this formulation, it is assumed that the heat of reaction of the solid-gas phase reaction affects the solid temperature only while that of occurring solely in the gas phase affects the gas phase temperature only. Also, the extent of swelling of the coal particles is directly proportional to the extent of devolatilization. Furthermore, the expression giving the gasification rate of the solid species CH_x (semichar) is somewhat complex. This rate is dependent on the time-temperature history of the particle and involves a double integration. The mathematical manipulation performed to simplify the complexity resulted into several additional differential equations, the details of which are given by Goyal (1).

The solid species production rate (S_1) is given by equation (18). The gas species production rates can be related to the solid species production rates (1).

Furthermore, coal hydrogenation experiments in the laboratory are often carried out in helical reactors (4, 6). The relationship between the particle

and the gas velocity is often represented in terms of a slip velocity factor (ϕ_g). In such reactor, the centrifugal forces are often more important than gravitational force. This slip velocity factor depends on the tube diameter, helix diameter, solids to gas ratio, particle size, gas velocity, etc. Thus for helical reactors:

$$D(v_s) = \phi_s D(v_g) \quad (24)$$

This equation replaces equation (5) in Table 2.

This set of equations (Table 2) also requires a large number of auxiliary, algebraic equations as component model parts; for example relationships for f_s , f_w , h_{gp} , h_{gw} , ϵ_{app} etc. These relationships are taken from the literature and the details are given by Goyal (1).

Furthermore, the model has been developed here for coal hydrolysis. Nevertheless, the formulations and the method of solution are flexible and can be easily manipulated for other entrained flow gasifiers, for example, peat gasification.

Solution Methodology

The entrained flow hydrolysis reactor has been modeled in the preceding section by a set of fifty three simultaneous nonlinear first order ordinary differential equations. The solutions to the formulations are sought in the form of time histories of quantities such as particle and gas temperature, their compositions, velocities, densities, and other derived quantities such as conversion etc. This system of equations is very stiff primarily due to the high temperature dependence of various hydrolysis reactor rates (1). A computer program based on implicit backward differentiation formulas of orders one through five (Gear's method) has successfully been used here in solving this set of stiff equations.

Comparison With Experimental Data

Cities Service Research and Development Company has performed studies on the hydrolysis of Montana Rosebud subbituminous coal, Western Kentucky No. 9/14 bituminous coal, and North Dakota lignite. Experiments were conducted in a bench-scale system of 2-4 lb/hr nominal capacity entrained-downflow tubular reactor. Different types of reactors (free fall, vertically-entrained, helically-entrained) were used in this study. The reactor was mounted inside an electric furnace designed for isothermal operation. Preheated hydrogen and coal were mixed inside a high-velocity coaxial injector nozzle located near the entrance to produce very high heating rates. The coal-hydrogen mixture moved to the reactor outlet where it was quenched to below 1000°F directly by a stream of cryogenically-cooled hydrogen, which terminated reactions. A more detailed description of the reactor system has been given by Hamshar et al. (7).

The reactor and coal types, flow rates, and operating conditions used in different test runs have been summarized along with experimental results by Cities Service Research and Development Co. (6). Operating conditions were varied in the nominal ranges of 1400°-1700°F reactor temperature, 34-170 atm reactor pressure, 0.18-1.3 hydrogen/coal weight ratio, and 0.3-25 sec vapor residence time. A few runs utilized a 78/22 (vol.) mixture of hydrogen/methane feed gas; the remainder used high purity hydrogen. The reactor temperature was measured by a series of removable skin thermocouples tacked along the wall of the reactor. However, these measured temperature profiles have not been reported. Instead, the mix temperature, maximum gas temperature and equivalent isothermal temperature for each run have been reported.

A total of twenty-one runs having good carbon and ash balance closures have been simulated in this study. The operating conditions for these runs are given by Goyal (1). The coal feed in these runs was dry. Also, several of their tests were conducted in helical coil reactors. Oko et al. (8) from Cities Service have recently reported the results of a helical glass cold-flow study. In this apparatus, average particle velocities were measured in the same flow regimes that were experienced in the bench-scale hydropyrolysis apparatus. The following empirical equation was derived to estimate the slip velocity factor:

$$\bar{\phi}_s = \bar{v}_s / \bar{v}_g = 1 - k_o \text{ Reg}_{R_c}^{p,q} (D_H/D_c)^r \quad 25)$$

where k_o , p , q , and r are empirical constants.

Several important reactor performance parameters have been compared here in Figures 1 through 4. Figure 1 shows a comparison of calculated and experimental carbon conversion for different types of coals. As seen from this figure, the computer model calculations agreed quite closely with the actual experimental results. Figure 2 compares the predicted moisture-ash-free (MAF) coal conversions with the experimental values of these conversions. The comparison is quite good; however, the model somewhat underpredicts this coal conversion. This is primarily due to the fact that Johnson's model allows for only 89% of coal oxygen evolution whereas the experimental oxygen evolution is approximately 97%. If this additional oxygen were allowed to evolve, then the predicted coal conversion would increase by approximately 1.5%. This would result in an excellent comparison.

Figure 3 compares the predicted carbon conversion to light hydrocarbons methane + ethane with experimental values. The predicted methane + ethane yield is somewhat higher. The comparison of carbon oxides yield is shown in Figure 4. The model underpredicts this yield. Again, it is probably because Johnson's model allows for only 89% coal oxygen removal while reported coal oxygen removal is in the range of 95% to 100%.

As mentioned earlier, the model is capable of predicting time histories of quantities such as conversions, particle and gas temperatures, their flow rates, compositions, velocities, etc. As an example, some of the important reactor variables have been summarized (as a function of reactor length) in Figures 5 to 7 for Run No. KB-5 with Western Kentucky bituminous coal feed. In this test, a 17.7 ft long and 0.26 inch ID reactor was operated at 1557°F (EIT) and 1500 psia hydrogen pressure. The superficial gas velocity, vapor residence time and hydrogen/coal weight ratio were 12.3 ft/sec, 1.44 sec, and 1.17 respectively. The wall temperature was assumed to be 1581°F which is the average of reported maximum reactor temperature and EIT. The data points shown in these figures are the actual experimental results at the reactor's exit.

Figure 5 shows carbon and MAF coal conversions as a function of reactor length. As seen from the figure, a significant conversion (12% to 14%) takes place within 0.1 ft reactor length. Note that the reactor length has been shown on a log scale, which allows to show the significant conversions occurring in the extremely short distance near the entrance. The particle residence time is also calculated by the model and is shown at the top of the graph.

Figure 6 shows the carbon conversion to different species over the length of the reactor. It shows that oil is evolved first and very rapidly. Again, log scale has been used to represent the reactor length. The change in the gas composition over the reactor length is shown in Figure 7. Pure hydrogen feed gas was used in this test and 96% of the exit product gas was hydrogen. This is so because excess amount of hydrogen was used in this run.

The mathematical model developed here has been used successfully to describe these hydrolysis reactors. Reasons for small discrepancies in experimental and predicted reactor performances are attributable to inadequacies in model formulation, unavailability of experimental data particularly reactor wall temperature profiles, and uncertainties in the experimental data.

A detailed parametric study has been performed using this model to identify important reactor parameters for the design of commercial entrained flow hydrolysis reactors. The results are given elsewhere (1).

Acknowledgement

The authors are grateful to Dr. S. Weil for providing many helpful suggestions and criticisms throughout this entire study.

Nomenclature

a	Contact area between solids and gas per unit reactor volume
a	Number of carbon atoms per mole of gas species $(CH_2)_a$
A	Reactor cross-sectional area
b	Number of carbon atoms per mole of gas species $(CH)_b$
B_j	Rate of gas species j going from solid phase to gas phase (i.e. crossing boundary) per unit reactor volume
C	Fractional coal conversion (moisture-free)
C_{af}	Fractional coal conversion (moisture-ash-free)
C_{pgj}	Heat capacity of gas species j
C_{psi}	Heat capacity of solid species i
D	Derivative with respect to distance along reactor (x)
D_H	Helix diameter
D_p	Particle diameter
D_t	Reactor diameter
f_s	Drag force exerted by fluid on the particles per unit volume of particles
f_w	Frictional force between the gas and the wall of the reactor
F	Solids flow rate per unit reactor cross-sectional area
g	Gravitational acceleration
g_c	Conversion factor (32.2 lbm-ft/sec ² /lbf)
G	Gas flow rate per unit reactor cross-sectional area
h_{gj}	Total enthalpy of gas species j
h_{gp}	Overall heat transfer coefficient between gas and solid particle
h_{gw}	Overall heat transfer coefficient between gas and wall
h_{si}	Total enthalpy of solid species i
H_{2gs}	Rate of gaseous hydrogen reacting with solid phase per unit reactor volume
H_{1s}	Wall heat losses from reactor per unit reactor length (due to convection between gas and wall)

H_{lsa}	Total wall heat losses from reactor per unit reactor length per unit reactor cross-sectional area
M	Atomic ratio of hydrogen to carbon in oils and tars (also in species CH_M)
M_j	Molecular weight of gas species j
P	Total reactor pressure
Q_{ash}	Ash flow rate per unit reactor cross-sectional area
R	Universal gas constant
R_c	Char to gas weight ratio
Re_g	Gas Reynolds number
R_i	Reaction rate ($d\xi_i/dt$) for i^{th} reaction
$(S_i)_s$	Mass rate of solid species i produced per unit reactor volume
$(S_j)_g$	Mass rate of gas species j produced per unit reactor volume
t	Time
T_g	Gas temperature
T_s	Solids temperature
T_w	Wall temperature
v_g	Gas velocity
v_s	Solids velocity
V_R	Ratio of particle volume at anytime to its initial volume
x	Distance along reactor
x	Atomic ratio of hydrogen to carbon in species CH_x (semichar)
y	Atomic ratio of hydrogen to carbon in species CH_y (final product char)
y_j	Mass fraction of gas species j
z	Atomic ratio of hydrogen to carbon in hydrocarbon gases other than CH_4 and C_2H_6 (also in solid species CH_2)
θ	Angle between horizontal line and the reactor axis
θ_g	Gas residence time
θ_s	Solids residence time
ρ_{ash}	Ash density
ρ_{ash}^o	Ash density of raw coal
ρ_g	Gas density
ρ_s	Solids density
ϵ	Voidage
ϵ_{app}	Effective emissivity
σ_B	Stephen-boltzman constant
γ_s	Swelling parameter

- ξ_i Fraction of solid species i not yet gasified ($i \neq \text{CH}_y$)
- $\xi_i^\circ = 1$ for $i \neq \text{CH}_y$
- $\omega_{\text{CH}_y}^\circ$ Maximum lbs of CH_y that can be formed per lb of ash (equation 21)
- ω_i° Lbs of solid species i in raw coal per lb of ash ($i \neq \text{CH}_y$)
- ϕ_s Slip velocity factor defined as the ratio of solids velocity to gas velocity

Subscript

- i Refers to solid species
- j Refers to gas species

References

- (1) Goyal, A., Mathematical Modeling of Entrained-Flow Coal Gasification Reactors, Ph.D. Thesis, Illinois Institute of Technology, Chicago, IL, May (1980).
- (2) Johnson, J. L., ACS, Div. of Fuel Chem. Preprints, 20, No. 3, 61 (1975).
- (3) Johnson, J. L., ACS, Div. of Fuel Chem. Preprints, 22, No. 1, 17 (1977).
- (4) Johnson, J. L. and D. Q. Tran, "Kinetics of Devolatilization and Rapid-Rate Methane Formation," Final Report, AGA Project IU-4-11, GRI Contract No. 5010-322-0025, Report No. GRI-78/0049, Institute of Gas Technology, Chicago, IL, Nov. (1980).
- (5) Suuberg, E. M., W. A. Peters and J. B. Howard, Ind. Eng. Chem. Process Design Develop., 17, No. 1, 37 (1978).
- (6) Cities Service Research and Development Company, "Hydrogasifier Development for the Hydrane Process," Final Technical Progress Report, Feb. 1977 to July 1978, Subcontract to Rocketdyne Division of Rockwell International Corporation of DOE Contract No. EX-77-C-01-2518, Cranbury, NJ, July 31 (1978).
- (7) Hamshar, J. A., S. J. Bivacca and M. I. Greene, Paper presented at 71st Annual AIChE Meeting, Miami Beach, FL, Nov. (1978).
- (8) Oko, U. M., J. A. Hamshar, G. Cuneo and S. Kim, ACS, Div. of Fuel Chem. Preprints, 24, No. 3, 82 (1979).
- (9) Gidaspow, D., "Hyperbolic Compressible Two-Phase Flow Equations Based on Stationary Principles and the Fick's Law," in Two Phase Transport and Reactor Safety, edited by S. Kakac and T. N. Veziroglu, 1, p. 283, Hemisphere Publishing Corp., Washington, D. C. (1978).

Table 1. Solid and Gas Species

<u>Solid Species</u>	<u>Gas Species</u>
1. HOH	1. CO
2. O·O	2. CO ₂
3. OH	3. H ₂
4. CO	4. H ₂ O
5. COO	5. CH ₄
6. CHH	6. C ₂ H ₆
7. CH _z	7. (CH _z) _a
8. CH _M	8. (CH _M) _b
9. CH _x	9. Inert gas
10. CH _y	
11. Ash	

Table 2. Differential Equations Model

$$\text{Total Solids Mass Balance: } D[(1-\epsilon)\rho_s v_s] = \Sigma(S_i)_s = D(F) \quad 1)$$

$$\text{Total Gas Mass Balance: } D(\epsilon \rho_g v_g) = \Sigma(S_j)_g = D(G) \quad 2)$$

$$\text{Solids Species Balance: } D(Q_{ash} \omega_i \xi_i) = (S_i)_s \quad 3)$$

$$\text{Gas Species Balance: } D(\epsilon \rho_g v_g y_j) = (S_j)_g \quad 4)$$

$$\text{Constitutive Equation for the Mixture: (Ref. 9)} \\ -(1/2)D \left[|v_g - v_s| (v_g - v_s) \right] = f_w / \rho_s - g \sin \theta \quad 5)$$

$$\text{Mixture Momentum Balance: } g_c D(P) = (v_g - v_s) \Sigma(S_i)_s - (1-\epsilon)\rho_s v_s D(v_s) \\ - \epsilon \rho_g v_g D(v_g) - f_w - [\rho_s (1-\epsilon) + \rho_g \epsilon] g \sin \theta \quad 6)$$

$$\text{Solids Density: } D(\rho_s) = D[\Sigma(\omega_i \xi_i) \rho_{ash}^o / V_R] \quad 7)$$

$$\text{Gas Density: } D(\rho_g) = D[(P/RT_g)(\Sigma y_j / M_j)^{-1}] \quad 8)$$

Table 2. Differential Equations Model (Cont.)

Solids Phase Energy Balance:
$$D(T_s) = - \{ [(-H_{2gs})(h_{gH_2})_{T_g} + \Sigma(B_j)(h_{gj})_{T_s} + h_{gp} a(T_s - T_g) - 4\sigma_B \epsilon_{app}(T_w^4 - T_s^4)/D_t] / Q_{ash} + \Sigma(\omega_i^\circ (h_{si})_{T_s} D(\xi_i)) / [\Sigma(\omega_i^\circ \xi_i C_{psi})] \}$$
 9)

Gas Phase Energy Balance:
$$D(T_g) = [(-H_{2gs})(h_{gH_2})_{T_g} + \Sigma(B_j)(h_{gj})_{T_s} + h_{gp} a(T_s - T_g) - H_{1s}/A - \Sigma(h_{gj})_{T_g} (S_j)_g] / [\Sigma(Gy_j C_{pgj})]$$
 10)

Fractional Coal Conversion:
$$D(C) = D[1 - \Sigma(\omega_i^\circ \xi_i) / \Sigma(\omega_i^\circ \xi_i^\circ)]$$

$$= D[-\Sigma(S_i)_s / (Q_{ash} \Sigma(\omega_i^\circ \xi_i^\circ))] \}$$
 11)

Particle Relative Volume:
$$D(V_R) = D[(1 + \gamma_s C_{af})^3]$$
 12)

Average Particle Diameter:
$$D(D_p) = (D_p / 3V_R) D(V_R)$$
 13)

Gas Residence Time:
$$D(\theta_g) = 1/v_g$$
 14)

Particle Residence Time:
$$D(\theta_s) = 1/v_s$$
 15)

Total Heat Loss:
$$D(H_{1sa}) = H_{1s}/A - 4\sigma_B \epsilon_{app}(T_w^4 - T_s^4)/D_t$$
 16)

Useful Algebraic Equations:

$$\Sigma(S_i)_s = -\Sigma(S_j)_g$$
 17)

$$(S_i)_s = (1-\epsilon) \rho_{ash} \omega_i^\circ R_i$$
 18)

$$Q_{ash} = (1-\epsilon) v_s \rho_{ash}$$
 19)

$$G = \epsilon \rho_g v_g$$
 20)

$$\omega_{CH_y}^\circ = (M_{CH_y} / M_{CH_x}) \omega_{CH_x}^\circ$$
 21)

$$H_{1s} = \pi D_t h_{gw} (T_g - T_w)$$
 22)

$$C_{af} = C[\Sigma(\omega_i^\circ \xi_i^\circ) / \Sigma\{(\omega_i^\circ \xi_i^\circ) - 1\}]$$
 23)

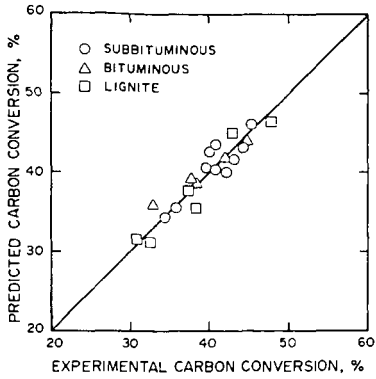


Figure 1. Comparison of Experimental and Predicted Carbon Conversion

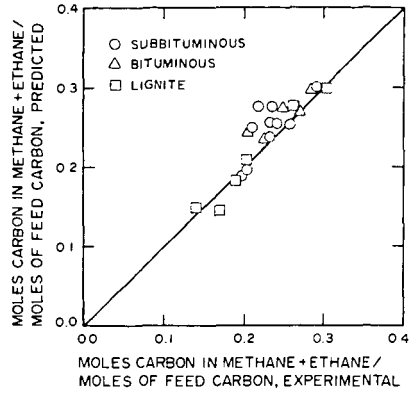


Figure 3. Comparison of Experimental and Predicted Methane + Ethane Yields

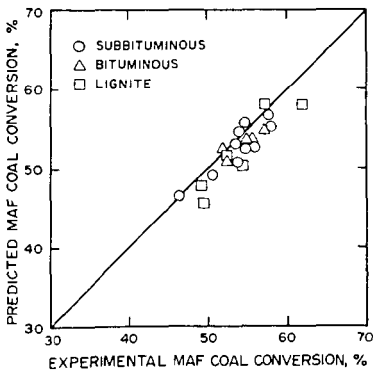


Figure 2. Comparison of Experimental and Predicted Moisture-Ash-Free Coal Conversion

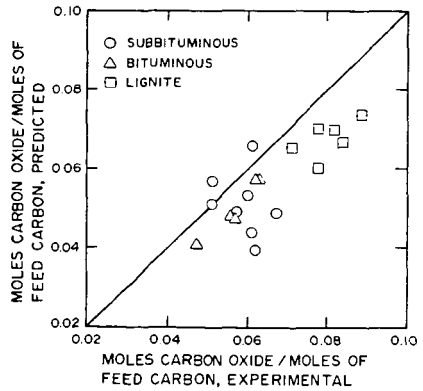


Figure 4. Comparison of Experimental and Predicted Carbon Oxides ($\text{CO} + \text{CO}_2$) Yields

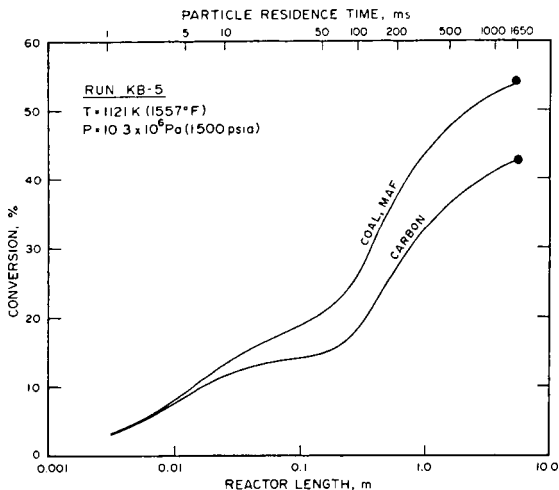


Figure 5. Carbon and Moisture-Ash-Free Coal Conversions along Reactor Length

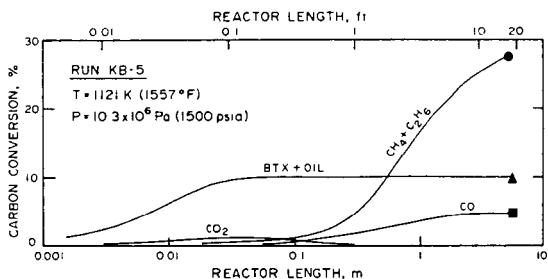


Figure 6. Distribution of Total Carbon Conversion to Different Species along Reactor Length

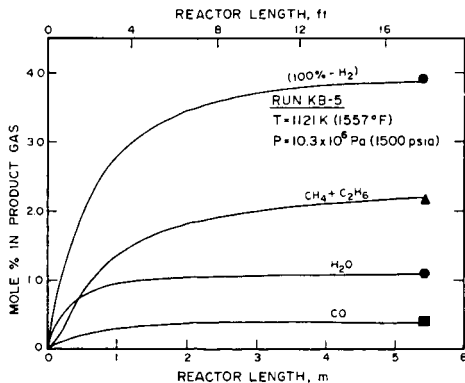


Figure 7. Gas Composition along Reactor Length